IET Renewable Power Generation

Research Article

IET Journals
The Institution of Engineering and Technology

Optimal wave energy extraction for oscillating water columns using second-order sliding mode control

ISSN 1752-1416
Received on 15th December 2019
Revised 18th February 2020
Accepted on 11th March 2020
E-First on 9th June 2020
doi: 10.1049/iet-rpg.2019.1392
www.ietdl.org

F. D. Mosquera[1] ✉, C. A. Evangelista[1], P. F. Puleston[1], J. V. Ringwood[2]

[1]Instituto LEICI, Facultad de Ingenieria, Universidad Nacional de La Plata and CONICET, La Plata, Argentina
[2]Department of Electronic Engineering, Centre for Ocean Energy Research, Maynooth University, Maynooth W23 F2H6, Ireland
✉ *E-mail: facundo.mosquera@ing.unlp.edu.ar*

Abstract: Ocean waves are an important renewable energy resource and several fields of *R&D* are concurrently working to improve technologies for harnessing their power. In that context, this study presents a control to optimise the performance of oscillating water column systems. As a first contribution, a novel criterion to attain maximum wave energy extraction is developed, resulting in an enhancement of the global power efficiency of the system. Then, taking advantage of the proposed criterion, a second-order sliding mode control set-up is designed, with power extraction maximisation the primary objective and reactive power regulation a secondary one. Simulation results confirm the highly satisfactory performance of the proposed controller and its robustness in the presence of the inherent uncertainties and disturbances in the non-linear system.

1 Introduction

The interest in clean renewable energy sources, essentially wind and solar, has grown relentlessly during the last decades. Recently, the international community has been paying attention to wave energy, which potentially would be capable of supplying a considerable part of the electricity demand in coastal areas [1]. Different technologies are being developed to harness this energy [2, 3], typically exploiting water surface movement or pressure variations produced below the water surface. An oscillating water column (OWC) system converts wave energy into mechanical energy by means of a semi-submerged chamber and a self-rectifying turbine (e.g. Wells turbine) [4]. Subsequently, the mechanical to electrical energy conversion is performed through a variable speed generator, for instance a double fed induction generator (DFIG), which has largely proven its suitability for variable speed operation in energy conversion applications [5–9].

Several criteria have been suggested to improve the conversion efficiency of OWC systems. In [10] and, more recently, in [7, 11], researchers have obtained very good results to increase wave energy extraction by regulating the rotational speed, computing the reference speed to avoid turbine stall. Another interesting approach has been introduced in [5, 12], where energy extraction enhancement is successfully achieved by operating at the flow coefficient of maximum turbine efficiency, which results in variable rotational speed operation. Then, the novel criterion developed in this paper naturally arises as a continuation of the aforementioned contributions, focusing on maximising the wave energy extraction, by considering the mechanical system as a whole.

Of particular appeal is a control approach capable of dealing with system uncertainties, unmodelled dynamics, external disturbances and non-linearities. Among the known techniques, sliding mode control (SMC) has proven to be an especially suitable approach to cope with such challenging specifications. In fact, since its origin [13–15], SMC has evolved into a powerful technique to design robust controllers for a broad range of non-linear applications [16–20]. In particular, [5, 11] recently proposed first-order SMC schemes for OWC systems, accomplishing highly satisfactory results. Motivated by their encouraging outcomes with first-order SMC, in this paper a second-order sliding mode (SOSM) control setup is developed. In years, the use of SOSM has successfully widened to many different applications [16–23]. This family of controllers, among other features, presents robustness and finite-time convergence, chattering amelioration (i.e. reduction of high-frequency oscillations of the controlled system, which sometimes appears in certain applications of first-order SMC), simple control laws with moderately low computational cost for implementation, and the possibility to be used in systems with relative degree (RD) 2, as in OWC systems. Specifically, in the proposed control set-up, a Twisting and a Super-Twisting SOSM algorithms are utilised together to fulfil the main control objective of maximum wave energy extraction and the secondary objective of reactive power regulation, respectively.

Main contributions of this paper are:

- Development of a new criterion for maximising wave energy extraction.
- Application of second-order SMC to an OWC system.

The remainder of the paper is organised as follows. Section 2 details the model of the complete system, comprising the OWC chamber, the Wells turbine and the DFIG. In Section 3, the novel criterion to attain maximum wave energy extraction is derived. In Section 4, the design of the proposed SOSM control set-up is presented. Representative simulation results are shown and analysed in Section 5 and, finally, conclusions are drawn in Section 6.

2 OWC model

This section presents the considerations for modelling the system under study and the resource. A representative scheme of the OWC system, integrated within a breakwater, is shown in Fig. 1.

2.1 Water wave mechanics

The most basic representation for a wave consists of a sinusoidal variation at the water surface elevation (monochromatic representation). This description can be defined by means of the wave height, H, which is the vertical distances from the wave crest to the wave trough, and the wave period, T, which is the time taken for the wave to repeat [24].

A more realistic characterisation is to consider that ocean waves vary randomly with time, with both height and period changing every moment. Therefore, to obtain representative attributes of a wave profile, a stochastic analysis has to be done, so that the wave spectral density, $S(\omega)$, can be obtained assuming a panchromatic

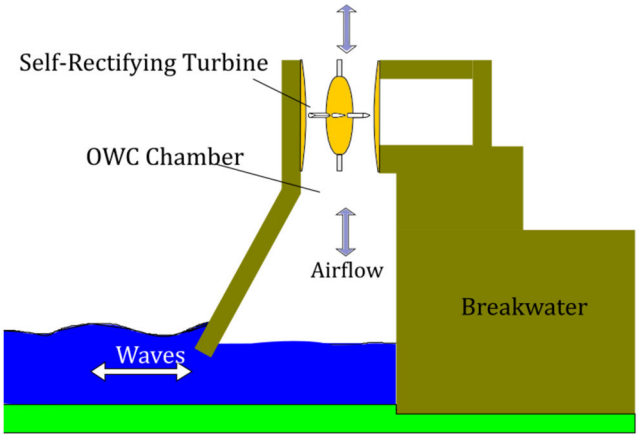

Fig. 1 *OWC system diagram*

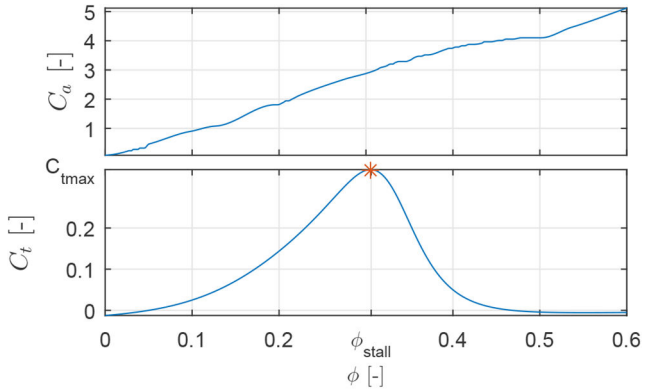

Fig. 2 *Top: power coefficient. Bottom: torque coefficient*

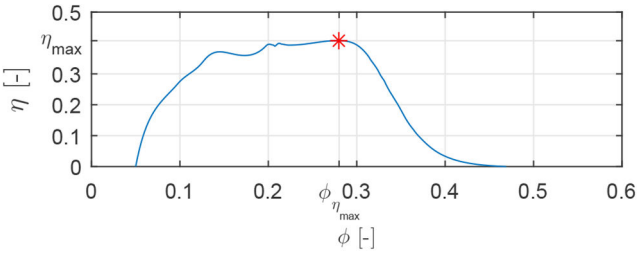

Fig. 3 *Turbine efficiency*

representation of the wave. One way to constitute the spectral density is by means of mathematical equations, which had been obtained empirically from observation of sea, then some properties can be used for building the spectrum of a particular wave climate. Among other representations have been the Pierson-Moskowitz, JONSWAP and Brestchneider spectra, each one modelling different origin of sea waves [25]. For illustrative purposes in this paper, wave based on a Pierson-Moskowitz spectral model is used, $S_{\mathrm{pm}}(\omega)$, which represents fully developed sea waves [26]

$$S_{\mathrm{pm}}(\omega) = \frac{0.11 H_{\mathrm{s}}^2 T_{\mathrm{z}}}{2\pi}\left(\frac{\omega T_{\mathrm{z}}}{2\pi}\right)^{-5} \mathrm{e}^{-0.44\left(\frac{\omega T_{\mathrm{z}}}{2\pi}\right)^{-4}} \tag{1}$$

where H_{s} is the significant wave height and T_{z} is the mean zero crossing wave period.

2.2 OWC chamber and self-rectifying turbine

The primary part of the converter is the capture chamber (see Fig. 1), which is composed of a fixed structure whose lower part is open to the sea below the still water level. The waves entering the chamber compress and decompress the air inside the structure so that an oscillating airflow is created. This airflow is passed through a power take-off system consisting of a turbine and a variable speed generator that transforms this motion into electrical power [27]. The bidirectional airflow inside the chamber (ν_t) is created by the interaction of the wave climate with the chamber geometry.

In order to convert bidirectional oscillating movement in unidirectional rotational movement, self-rectifying turbines are utilised, most are axial-flow machines of two basic types: Wells turbines and impulse turbines [1], though radial turbines are also emerging [28]. Wells turbines employ a rotor with symmetric blades staggered at 90° with respect to the incoming flow and are particularly interesting because of their simplicity of operation and reliability [29]. The equations used to model the turbine are described as follows [9]:

• Power available for the device

$$P_{\mathrm{in}} = q\,\Delta p\ [W] \tag{2}$$

where Δp [Pa] and q [m^3/s] are the pressure drop and the flow rate in the turbine, respectively.

• Flow rate

$$q = \nu_x a \tag{3}$$

where $\nu_x = |\nu_t|$ is the unidirectional airflow speed in the direction perpendicular to the blade area and a [m^2] is the area of the turbine duct. Note that ν_x is unidirectional because of the self-rectifying property of the turbine.

• Pressure drop

$$\Delta p = C_a(\phi) k \frac{1}{a}\left[\nu_x^2 + (r\Omega_r)^2\right] \tag{4}$$

where $k = \rho b n l/2$ [kg/m], ρ [kg/m^3] is the air density, b [m] is the blade length, n the number of blades and l [m] is the chord length. Ω_r [rad/s] is the turbine rotational speed and $C_a(\phi)$ is the power coefficient which is dependant on ϕ, the flow coefficient. A plot of a typical $C_a(\phi)$ profile can be observed in Fig. 2.

• Flow coefficient

$$\phi = \frac{\nu_x}{r\Omega_r} \tag{5}$$

where r [m] is the blade radius.

• Turbine torque

$$T_t = C_t(\phi) k r\left[\nu_x^2 + (r\Omega_r)^2\right] \quad [Nm] \tag{6}$$

where $C_t(\phi)$ is the torque coefficient, which also depends on ϕ (see Fig. 2). The effect of stall can be observed for $\phi > \phi_{\mathrm{stall}}$.

• Turbine efficiency

$$\eta = \frac{P_{\mathrm{out}}}{P_{\mathrm{in}}} = \frac{T_t \Omega_r}{q\Delta p} = \frac{C_t}{C_a \phi} \tag{7}$$

relates the mechanical output power to the available power due to pressure drop and flow rate. A typical graph of $\eta(\phi)$ is shown in Fig. 3.

2.3 System dynamics

The dynamic system behaviour can be described adequately by a set of five differential equations. Four of them are related to the electrical dynamics of the induction generator. In terms of the machine fluxes, and using two reference frames rotating at synchronous speed, for rotor and stator variables, respectively, they are [30]

$$\begin{cases} \dot{\psi}_{ds} &= v_{ds} - R_s i_{ds} + \omega_s \psi_{qs} \\ \dot{\psi}_{qs} &= v_{qs} - R_s i_{qs} - \omega_s \psi_{ds} \\ \dot{\psi}_{dr} &= v_{dr} - R_r i_{dr} + (\omega_s - p\,\Omega_r)\psi_{qr} \\ \dot{\psi}_{qr} &= v_{qr} - R_r i_{qr} - (\omega_s - p\,\Omega_r)\psi_{dr} \end{cases} \tag{8}$$

together with the following algebraic relations:

$$\begin{aligned} \psi_{ds} &= L_s i_{ds} + L_m i_{dr} \\ \psi_{qs} &= L_s i_{qs} + L_m i_{qr} \\ \psi_{dr} &= L_r i_{dr} + L_m i_{ds} \\ \psi_{qr} &= L_r i_{qr} + L_m i_{qs} \end{aligned} \tag{9}$$

where the state variables ψ_{qs}, ψ_{ds}, ψ_{qr} and ψ_{dr} represent the direct ($_d$) and quadrature ($_q$) flux components for stator and rotor, v_{qs}, v_{ds}, v_{qr} and v_{dr} (i_{qs}, i_{ds}, i_{qr} and i_{dr}) are the components of the voltages (currents). Also, R_s and R_r are the electric resistance of stator and rotor windings, respectively, L_s and L_r are the self-inductance of the respective windings, and L_m is the mutual inductance between the stator and rotor windings. p is the number of pole pairs and $\omega_s = 2\pi f_s$ is the synchronous frequency, where f_s is the grid frequency.

The mechanical dynamics are described by

$$J\dot{\Omega}_r = T_t - T_e \tag{10}$$

where J represents the inertia of the rotating parts, T_t is the turbine torque (6) and T_e is the generator torque, given by

$$T_e = -\frac{3}{2} p L_m \left(i_{dr} i_{qs} - i_{qr} i_{ds}\right) \tag{11}$$

where a negative sign is added in order to have a positive torque when the machine is working as a generator. Finally, the stator reactive power, Q_s, is

$$Q_s = \frac{3}{2}\left(v_{qs} i_{ds} - v_{ds} i_{qs}\right) \tag{12}$$

3 Proposed criterion for maximum wave energy extraction

A new criterion is presented in this section, developed by the authors to establish an optimum reference for the rotational speed, in order to achieve mechanical output power maximisation.

The criterion is obtained by expressing the power extracted by the Wells turbine as a product of two factors, one of them depending only on the wave, i.e. the external energy source, and the other a function of the flow coefficient. From (7), and using (2)–(4), the mechanical power in the turbine shaft can be written as

$$P_{\text{out}} = \eta P_{\text{in}} = \eta(\phi) C_a(\phi) \frac{k}{a} \left[\nu_x^2 + (r\Omega_r)^2\right] \nu_x a \tag{13}$$

Note that ν_x is an external variable, which is a function of the wave climate and the geometric characteristics of the OWC chamber, and independent of the rotational speed or any other state variable of the turbine [31]. Following some algebraic manipulation, the output power can be expressed as

$$P_{\text{out}} = \underbrace{\frac{2k}{\rho a}\eta(\phi) C_a(\phi)\left(1 + \phi^{-2}\right)}_{C_{P_f}(\phi)} \underbrace{\frac{\rho a}{2}\nu_x^3}_{P_f} = C_{P_f}(\phi) P_f(\nu_x) \tag{14}$$

where C_{P_f} is a dimensionless, non-linear function of ϕ, that relates the extracted power, P_{out}, to a fictitious power P_f, defined in correspondence with the kinetic power developed by the airflow passing through an area a at speed ν_x. Fig. 4 shows the graph of the

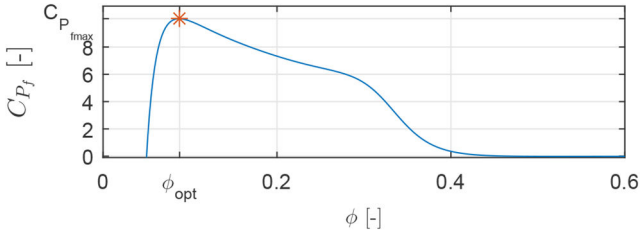

Fig. 4 *Coefficient $C_{P_f}(\phi)$*

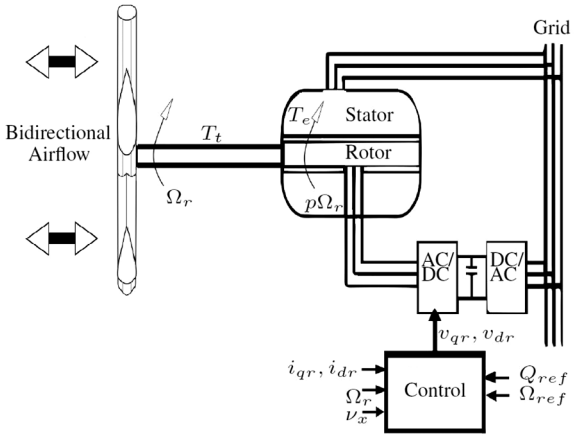

Fig. 5 *Schematic diagram of the controlled system*

$C_{P_f}(\phi)$ coefficient corresponding to the power coefficient $C_a(\phi)$ and the turbine efficiency $\eta(\phi)$ shown in Figs. 2 and 3.

Remark 1: It can be seen that $C_{P_f}(\phi)$ has a single maximum, at $\phi = \phi_{\text{opt}}$. Therefore, according to (14), the proposed criterion to maximise the power extracted by the turbine is to operate the system at $\phi = \phi_{\text{opt}}$.

Thus, the strategy is based on controlling the rotational speed so that this optimum condition is maintained for the varying input ν_x and, to this end, an optimum speed reference is defined as

$$\Omega_{\text{opt}} = \frac{\nu_x}{r\phi_{\text{opt}}} \tag{15}$$

4 SOSM controllers design

For this paper, the proposal is to accomplish two control objectives simultaneously. The main one is the maximisation of wave power extraction, in accordance with the criterion elaborated in Section 3. The secondary, but also important, objective focuses on reactive power control. A schematic representation of the controlled system is presented in Fig. 5.

As stated in the Introduction, the distinctive features of the SOSM techniques, applied to control electromechanical systems, make them an excellent choice for the system under study. Specifically, SOSM control defines a function of the system states, the so-called sliding variable σ, so that the control objectives are achieved when $\sigma = \dot{\sigma} = 0$. Such a condition defines the sliding surface in the state space, and SOSM algorithms are designed so that the system trajectories converge to it in finite time and robustly remain there, even in the presence of certain disturbances and uncertainties considered during the design stage [32–34].

The steps for the design of the OWC system SOSM control setup are addressed in the following subsection.

4.1 OWC system reduced model for the control design

Firstly, for designing purposes, a reduced order model of the system is presented, which is simpler while still retaining the essential system characteristics [8]

$$\begin{aligned}\dot{i}_{qr} &= \frac{L_s}{L_{eq}}(v_{qr} - R_r i_{qr}) - \left(i_{dr} + \frac{L_m V_s}{\omega_s L_{eq}}\right)(\omega_s - p\Omega_r)\\ \dot{i}_{dr} &= \frac{L_s}{L_{eq}}(v_{dr} - R_r i_{dr}) + i_{qr}(\omega_s - p\Omega_r)\\ \dot{\Omega}_r &= \frac{1}{J}\left(T_t(\nu, \Omega_r) - \frac{3pL_m V_s}{2\omega_s L_s} i_{qr}\right)\end{aligned} \tag{16}$$

where V_s is the grid phase voltage and $L_{eq} = L_s L_r - L_m^2$. The rotor fluxes are related to the rotor currents via

$$\psi_{qr} = \frac{L_{eq}}{L_s} i_{qr};\ \psi_{dr} = \frac{L_{eq}}{L_s} i_{dr} + \frac{L_m V_s}{\omega_s L_s} \tag{17}$$

and stator currents can be calculated as

$$i_{qs} = -\frac{L_m}{L_s} i_{qr};\ i_{ds} = \frac{V_s}{\omega_s L_s} - \frac{L_m}{L_s} i_{dr} \tag{18}$$

For the reduced model, the stator reactive power and the generator torque can be expressed as

$$Q_s = \frac{3pV_s^2}{2\omega_s L_s} - \frac{3pL_m V_s}{2L_s} i_{dr} \tag{19}$$

$$T_e = \frac{3}{2}\frac{pL_m V_s}{\omega_s L_s} i_{qr} \tag{20}$$

4.2 Selection of the sliding variables

Considering the structure of the reduced dynamic model, together with both desired goals, a selection of two sliding variables can be proposed which are input–output decoupled, i.e. each of the two control input components directly affects only one of the two sliding variables and not the other. Thus, from the SOSM design viewpoint, the control problem can be treated as two separated SISO systems.

4.2.1 Primary objective. Wave power extraction maximisation: A sliding variable σ_1 is defined in this section to maximise the energy extracted from the waves by the OWC system, to be achieved by tracking the optimal reference (15), derived in Section 3.

Evidently, from a theoretical perspective, the best result would be obtained if the flow coefficient were permanently kept at the optimum value ϕ_{opt} for all ν_x (i.e. $\Omega_{\text{ref}} = \Omega_{\text{opt}}(\nu_x)$). However, this would be impractical, given that it would periodically force the turbine to stop, which is mechanically undesirable.

To avoid this behaviour, a sub-optimal solution is implemented, defining a piecewise reference limited by a minimum-speed threshold, $\Omega_{r_{\min}}$

$$\Omega_{\text{ref}} = \begin{cases}\Omega_{\text{opt}}(\nu_x) = \dfrac{\nu_x}{r\phi_{\text{opt}}}, & \text{if } \Omega_{\text{opt}}(\nu_x) > \Omega_{r_{\min}}\\ \Omega_{r_{\min}}, & \text{if } \Omega_{\text{opt}}(\nu_x) \le \Omega_{r_{\min}}\end{cases} \tag{21}$$

According to (21), the sliding variable for the first control objective is defined as

$$\sigma_1 = \Omega_{\text{ref}} - \Omega_r \tag{22}$$

4.2.2 Secondary objective. Reactive power regulation: The second sliding variable, σ_2, is defined so that the stator reactive power tracks an external reference $Q_{\text{ref}}(t)$. Then, using (19)

$$\sigma_2 = Q_{\text{ref}} - Q_s = Q_{\text{ref}} - \frac{3pV_s^2}{2\omega_s L_s} + \frac{3pL_m V_s}{2L_s} i_{dr} \tag{23}$$

4.3 Design of the SOSM controllers

It is straightforward to determine that σ_1 is of RD 2 with respect to v_{qr} (not depending on v_{dr} up to the second derivative, $\ddot{\sigma}_1$), while σ_2 is of RD 1 with respect to v_{dr} (not depending on v_{qr} up to the first derivative, $\dot{\sigma}_2$). Then, two different SOSM algorithms, Twisting and Super-Twisting, suitable for RD 2 and RD 1 systems, respectively, have been chosen.

4.3.1 Wave power extraction maximisation controller: The following two-term v_{qr} control action is proposed to robustly fulfil the primary control objective

$$v_{qr} = v_{qr_E} + v_{qr_T} \tag{24}$$

The first term, v_{qr_E}, is a continuous 'bias' control action designed to steer the system to the neighbourhood of $\sigma_1 = 0$. The second term, v_{qr_T}, is the SOSM Twisting control action, which provides robustness to uncertainties and disturbances. Note that v_{qr_E} has been included to reduce the control effort demanded by the SOSM action. Its presence results in the design of smaller gains for the SOSM controller (hence, lesser discontinuous action and chattering), while still ensuring the existence of a robust sliding mode regime.

Firstly, the 'bias' control term v_{qr_E} is derived following a procedure inspired by the equivalent control concept in SMC systems. The RD 2 sliding variable σ_1 is differentiated until the control v_{qr} explicitly appears

$$\begin{aligned}\ddot{\sigma}_1 = &\underbrace{\ddot{\Omega}_{\text{ref}} - \frac{\dot{T}_t}{J} + \frac{1}{J}\frac{3pL_m V_s}{2\omega_s L_s}\left(R_r i_{qr} + \psi_{dr}(w_s - p\Omega_r)\right)}_{a_1(x,t)}\\ &+\underbrace{\frac{1}{J}\frac{3pL_m V_s}{2\omega_e L_{eq}}}_{b_1(x,t)} v_{qr} = a_1(x,t) + b_1(x,t) v_{qr}\end{aligned} \tag{25}$$

where $x = [i_{qr}; i_{dr}; \Omega_r]$ denotes the states. Then, the expression of v_{qr_E} can be easily obtained from (25), as the continuous control that ensures $\sigma_1 = \dot{\sigma}_1 = \ddot{\sigma}_1 = 0$

$$v_{qr_E} = v_{qr}\Big|_{\sigma_1 = \dot{\sigma}_1 = \ddot{\sigma}_1 = 0} = -\frac{a_1(x,t)}{b_1(x,t)}\Big|_{\sigma_1 = \dot{\sigma}_1 = \ddot{\sigma}_1 = 0} \tag{26}$$

assuming that the system is undisturbed, i.e. neither uncertainties nor unknown disturbances exist.

Secondly, the SOSM Twisting control term, of the form [35]

$$v_{qr_T}(\sigma_1) = -r\,\text{sign}(\sigma_1) - r'\,\text{sign}(\dot{\sigma}_1), \quad r > r' > 0, \tag{27}$$

is designed.

To tune the control gains r and r' in accordance with the Twisting algorithm procedure, $\ddot{\sigma}_1$ needs to be explicitly written in terms of the SOSM control v_{qr_T} in the general form

$$\ddot{\sigma}_1 = \lambda_1(x,t) + \gamma_1(x,t) v_{qr_T}. \tag{28}$$

Hence, substituting (24) into (25) gives

$$\ddot{\sigma}_1 = \underbrace{a_1(x,t) + b_1(x,t) v_{qr_E}}_{\lambda_1(x,t)} + \underbrace{b_1(x,t)}_{\gamma_1(x,t)} v_{qr_T} \tag{29}$$

Then, functions $\lambda_1(x,t)$ and $\gamma_1(x,t)$ must be bounded with three positive constants $\Gamma_{m_1} < \Gamma_{M_1}$ and C_1, that satisfy

$$\begin{aligned}|\lambda_1(x,t)| &\le C_1\\ \Gamma_{m_1} \le \gamma_1(x,t) &\le \Gamma_{M_1}\end{aligned} \tag{30}$$

Table 1 System parameters

Turbine and chamber	Generator	
$n = 5$	$p = 1$	$R_r = 0.2305\ \Omega$
$l = 0.165$ m	$J_g = 0.07$ kg m^2	$L_s = 1.7$ mHy
$b = 0.21$ m	$P = 7.5$ kW	$L_r = 2.4$ mHy
$r = 0.375$ m	$V_{rms} = 400\ V_{rms}$	$L_m = 76.6$ mHy
$l_c = 4.3$ m	$f_s = 50$ Hz	
$w = 4.5$ m	$\omega_s = 2\pi f_s$ rad/s	
$J_p = 0.44$ kg m^2	$R_s = 0.2702\ \Omega$	

Note that, to attain robust performance, the disturbances and uncertainties should be contained within these bounds. Finally, the gains must be chosen according to the following sufficient conditions to guarantee finite time convergence to $\sigma_1 = \dot{\sigma}_1 = 0$

$$\begin{aligned} r &= r' + \Delta_T \\ r' &> \frac{\Delta_T(\Gamma_{M_1} - \Gamma_{m_1}) + 2C_1}{2\Gamma_{m_1}} \\ \Delta_T &> \frac{C_1}{\Gamma_{m_1}} \end{aligned} \tag{31}$$

4.3.2 Reactive power regulation controller: To robustly accomplish the secondary objective of reactive power regulation, a two-term control law is proposed as well

$$v_{dr} = v_{dr_E} + v_{dr_{ST}}, \tag{32}$$

comprising a smooth 'bias' control term v_{dr_E} and a SOSM Super-Twisting term $v_{dr_{ST}}$. The Super-Twisting algorithm was chosen because it can be directly applied to the RD 1 sliding variable σ_2. Additionally, it provides a continuous control action (which further improves the chattering amelioration) and does not rely on knowledge of $\dot{\sigma}_2$. A procedure, analogous to the one utilised in the previous case, is followed to obtain the control terms, bearing in mind that σ_2 is of RD 1 instead of 2.

Firstly, the 'bias' control v_{dr_E} is computed. In this case, the control action v_{dr} explicitly appears in the first time derivative of σ_2

$$\begin{aligned} \dot{\sigma}_2 = \underbrace{\dot{Q}_{\text{ref}} - \frac{3pV_sL_m}{2\omega_sL_{eq}}\left(R_r\dot{i}_{dr} - \psi_{qr}(\omega_s - p\Omega_r)\right)}_{A_2(x,t)} + \\ + \underbrace{\frac{3pV_sL_m}{2\omega_sL_{eq}}}_{B_2(x,t)} v_{dr} = A_2(x,t) + B_2(x,t)v_{dr}, \end{aligned} \tag{33}$$

and, from (33), the smooth control v_{dr_E} that guarantees $\sigma_2 = \dot{\sigma}_2 = 0$ results in the form

$$v_{dr_E} = v_{dr}\Big|_{\sigma_2 = \dot{\sigma}_2 = 0} = -\frac{A_2(x,t)}{B_2(x,t)}\Big|_{\sigma_2 = \dot{\sigma}_2 = 0} \tag{34}$$

considering the undisturbed, or nominal, system.

Secondly, the robust SOSM Super-Twisting term $v_{dr_{ST}}$ is introduced [35]

$$v_{drST}(\sigma_2) = -\beta\left|\sigma_2\right|^{\frac{1}{2}}\text{sign}(\sigma_2) - \alpha\int_0^t \text{sign}(\sigma_2(\tau))\text{d}\tau \tag{35}$$

where β and α are the control gains.

The tuning of the Super-Twisting gains requires $\ddot{\sigma}_2$ to be expressed explicitly in terms of $\dot{v}_{dr_{ST}}$ as

$$\ddot{\sigma}_2 = \lambda_2(x, v_{qr}, v_{dr}, t) + \gamma_2(x,t)\dot{v}_{dr_{ST}}. \tag{36}$$

Consequently, differentiating the σ_2 twice

$$\begin{aligned} \ddot{\sigma}_2 = \underbrace{\ddot{Q}_{\text{ref}} - \frac{3pL_mV_s}{2w_sL_{eq}}\frac{\text{d}}{\text{d}t}\left(R_r\dot{i}_{dr} - \psi_{qr}(\omega_s - p\Omega_r)\right)}_{a_2(x, v_{qr}, v_{dr}, t)} \\ + \underbrace{\frac{3pV_sL_m}{2\omega_sL_{eq}}}_{b_2(x,t)}\dot{v}_{dr} = a_2(x, v_{qr}, v_{dr}, t) + b_2(x,t)\dot{v}_{dr} \end{aligned} \tag{37}$$

and substituting (32) into (37), it gives

$$\ddot{\sigma}_2 = \underbrace{a_2(x, v_{qr}, v_{dr}, t) + b_2(x,t)\dot{v}_{dr_E}}_{\lambda_2(x, v_{qr}, v_{dr}, t)} + \underbrace{b_2(x,t)}_{\gamma_2(x,t)}\dot{v}_{dr_{ST}} \tag{38}$$

as required in (36).

To complete the Super-Twisting design procedure, functions $\lambda_2(x, v_{qr}, v_{dr}, t)$ and $\gamma_2(x,t)$ must be bounded with three positive constants $\Gamma_{m_2} < \Gamma_{M_2}$ and C_2 such that

$$\begin{aligned} \left|\lambda_2(x, v_{qr}, v_{dr}, t)\right| &\leq C_2 \\ \Gamma_{m_2} \leq \gamma_2(x,t) &\leq \Gamma_{M_2}, \end{aligned} \tag{39}$$

taking into account the disturbances and uncertainty bounds.

Finally, if the gains are selected so that they verify the sufficient conditions

$$\begin{aligned} \alpha &> \frac{C_2}{\Gamma_{m_2}} \\ \beta &> \frac{\sqrt{2(\alpha\Gamma_{M_2} + C_2)}}{\Gamma_{m_2}}, \end{aligned} \tag{40}$$

then, finite-time convergence to $\sigma_2 = \dot{\sigma}_2 = 0$ and robust SOSM operation are guaranteed, even in the presence of disturbances and uncertainties considered in the computation of the bounds.

5 Simulations results

The results obtained with the new criterion for maximum wave energy extraction, together with the proposed SOSM control setups, are presented and analysed in this section in two representative cases. In case study 1, a realisation of a panchromatic wave with Pierson-Moskowitz spectrum was utilised to assess the controller's behaviour under a realistic wave climate. In case study 2, the maximum wave energy extraction criterion proposed is contrasted with other criteria for energy extraction, using a train of perturbed monochromatic waves which allows a clear comparison.

To test the controllers under practical conditions, the simulations are conducted utilising the full order model of the OWC system (8)–(12), incorporating uncertainties up to 15% with respect to the electrical and aerodynamic parameters. The parameters of the Wells turbine, chamber and the 7.5 kW DFIG generator are shown in Table 1.

The disturbed model was considered to compute the bounding constants in (30) and (39). Practical bounds were obtained through exhaustive analysis under realistic conditions of operation and assisted by comprehensive computer simulations. After further heuristic refinement, the following gains, suitable for practical use, have been set for the controllers:

$$\begin{aligned} r = 20; \quad r' = 10 \\ \alpha = 596.5; \quad \beta = 3.88 \end{aligned}$$

5.1 Case study 1: irregular waves

The present case considers the use of a Pierson-Mozkowitz spectrum with $H_s = 0.9$ m and $T_z = 12$ s, which models a realistic wave climate. Thus, the simulations presented herein correspond to the ariflow profile shown in Fig. 6.

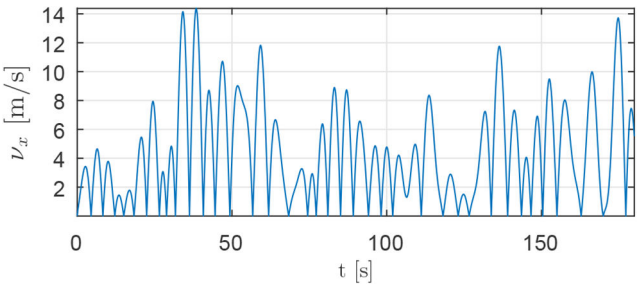

Fig. 6 *Airflow speed*

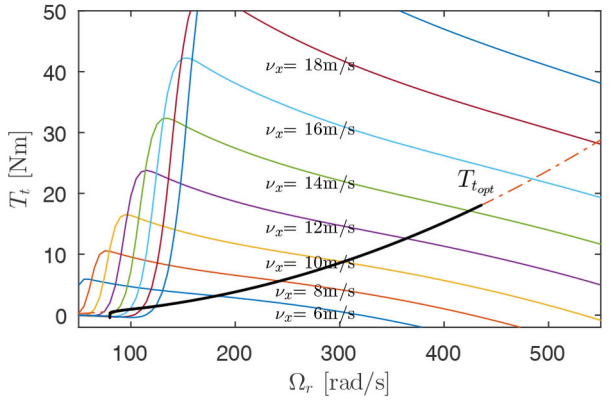

Fig. 7 *System characteristic curve (solid black line) in the $T_t - \Omega_r$ plane. Locus of maximum wave power extraction (dot-dashed line). Turbine characteristics for ν_x (solid coloured lines)*

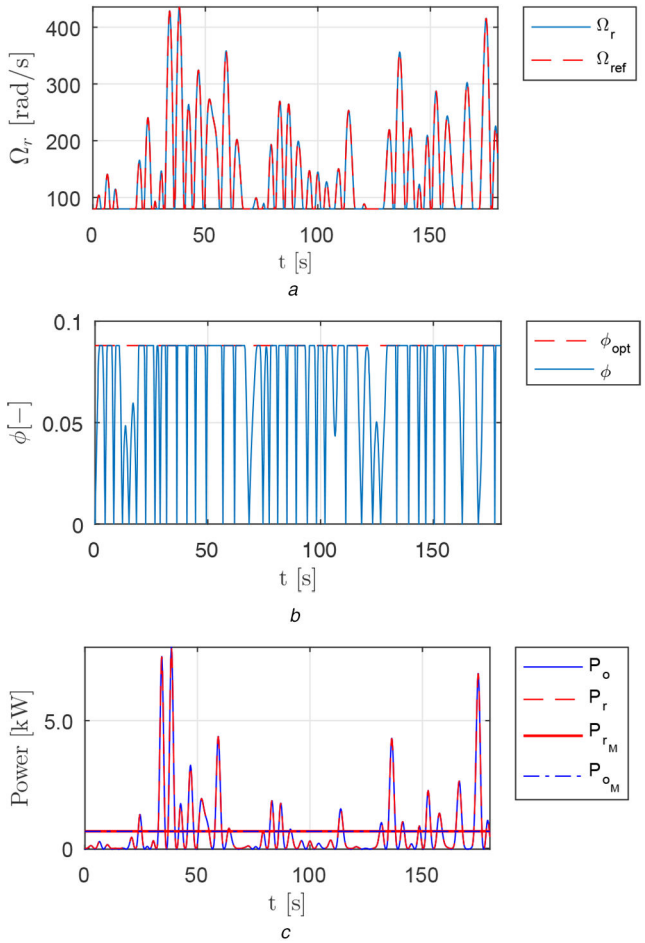

Fig. 8 *First control objective: wave power extraction*
(a) Rotational speed, ***(b)*** Flow coefficient, ***(c)*** Wave power extracted

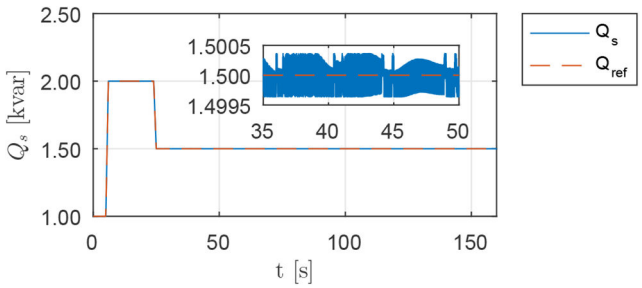

Fig. 9 *Second control objective: stator reactive power*

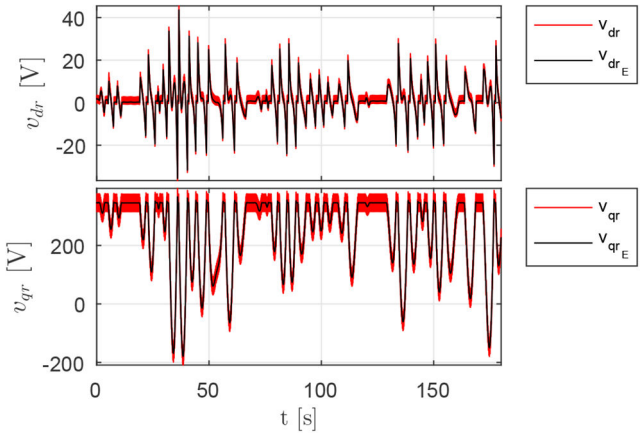

Fig. 10 *Control actions (solid red lines) and smooth 'bias' terms (solid black lines)*

The behaviour of the mechanical torque of the turbine, T_t, is shown in the torque–speed plane in Fig. 7. The figure also presents the locus of maximum wave power extraction of the system, indicated as T_{opt}. As can be appreciated, above the minimum-speed threshold $\Omega_{r_{\min}}$ (79.86 rad/s), the SOSM control setup succeeds in maintaining the turbine operating at the optimum reference, despite the uncertainties.

Results related to the primary objective of wave power extraction maximisation are shown in Fig. 8. Firstly, Fig. 8*a* displays the turbine rotational speed Ω_r and its reference Ω_{ref}, showing the excellent tracking features of the proposed controller. Accordingly, Fig. 8*b* depicts the flow coefficient, which is maintained at the desired optimum value ($\phi_{\text{opt}} = 0.088$ for the system under study) while the turbine is rotating above $\Omega_{r_{\min}}$. On the other hand, ϕ follows ν_x when the Ω_r is kept constant at $\Omega_{r_{\min}}$. Lastly, in Fig. 8c, the wave power extracted is presented (solid blue line), with a peak value of 7.87 kW and a mean value equal to 663 *W* (dot-dashed blue line). It can be observed that the extracted power practically matches the theoretical maximum P_r (dashed red line), obtained by assuming ideal operation at $\phi = \phi_{\text{opt}}$ during the complete test run.

The accomplishment of the secondary control objective can be appreciated in Fig. 9, where the stator reactive power and the external reference Q_{ref} are depicted together. The two curves are almost overlapped, proving the robust tracking features of the control set-up. The zoom box inside shows that the error (i.e. σ_2) is negligible, remaining below 0.05%, during the complete test.

Fig. 10 presents the control inputs, consisting of the rotor voltages v_{qr} and v_{dr} (Fig. 10, top and bottom, respectively) of the DFIG (solid red lines), and the 'bias' controls of v_{qr_E} and v_{dr_E} (dash-dotted black line). It is noticeable that the 'bias' terms, calculated with the nominal values of the model, make the primary contribution to the total control action. Then, the SOSM controls only have to deal with the disturbances and modelling errors. This results in a robust control action with small sliding mode gains.

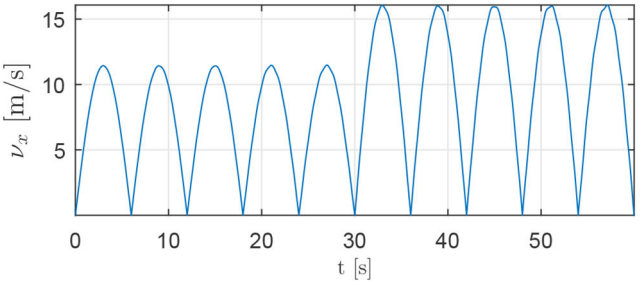

Fig. 11 *Airflow speed*

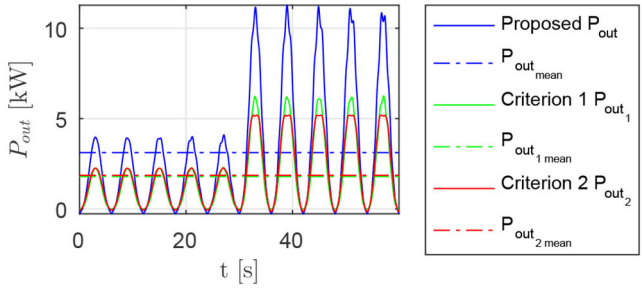

Fig. 12 *Wave extracted power with different criteria*

5.2 Case study 2: regular waves

In this case, a comparison between the proposed control criterion and two previous reported comparable criteria [5, 11] is displayed. For a clear visualisation of the comparison results, a wave profile composed of two consecutive trains of perturbed monochromatic waves has been used. The first half of the wave signal has a mean wave period of $T = 12$ s, and a mean wave height of $H = 1$ m. After a transition, at $t = 30$ s, the mean wave height is increased, resulting into a 40% airflow amplitude increase (as depicted in Fig. 11).

For the sake of illustration, the extracted power (P_{out}) obtained with the novel criterion proposed in Section 3, is depicted in Fig. 12, together with the ones obtained with the two reference criteria. The first one, Criterion 1 (solid red line), proposes operation at maximum turbine efficiency (eq. (7), Fig. 3), which is accomplished by maintaining the flow coefficient constant at $\phi = \phi_{\eta_{\max}} = 0.29$ (for the system under study). The second one, Criterion 2 (solid green line), aims to increase wave energy extraction by regulating the rotational speed to avoid turbine stall. To this end, the reference speed is computed in accordance with $\phi_{\text{stall}} = 0.3$ (see Fig. 2) and two different values of Ω_{ref}, 105.19 and 124.32 rad/s, respectively, for the two portions of the simulation interval. It should be noted that, due to the lower rotational speed ranges of criteria 1 and 2, a DFIG with two pairs of poles ($p = 2$) was used for the corresponding tests.

Finally, the electrical energy delivered to the grid by each criterion is shown in Fig. 13. To illustrate, a period of 10 min, which comprises several wave cycles, has been depicted.

6 Conclusions

Two main conclusions can be drawn from this work. The first one is that to increase power extraction from the waves, it is necessary to approach the OWC system as a whole. In this sense, excellent results have been obtained with the novel criterion introduced in the paper. The underlaying rationale for its development, was to express the power extracted by the turbine as a product of two factors, one depending only on the wave (external energy source) and the other a function of the flow coefficient (a system variable). In this way, wave energy maximisation is reduced to a very simple objective, to operate at the flow coefficient that maximises the extracted power. It should be added that the control objective, shaped in accordance with the proposed criterion, not only appropriate with SMC, but also with other different control techniques of interest.

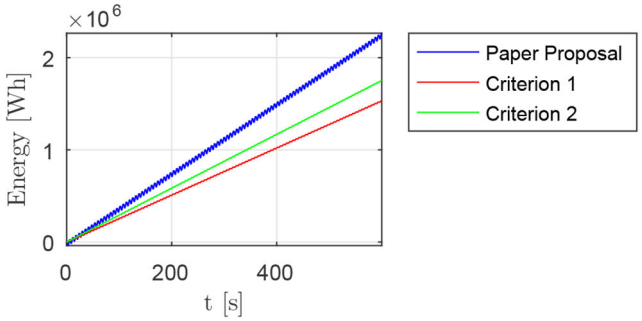

Fig. 13 *Electrical energy generated in 10 min*

The second noteworthy conclusion is that it has been shown that SOSM techniques are especially suitable to tackle the control challenges presented by OWC systems. In effect, highly successful simulation results have been achieved with the SOSM control setups designed in this paper. Based on the Twisting and Super-Twisting algorithms, the objectives of wave power extraction maximisation and reactive power regulation have been robustly attained, even in a non-linear system with uncertainties and an extremely varying input, as a typical wave train is.

7 Acknowledgment

This work has been supported by the Universidad Nacional de La Plata, the CONICET and the Agencia Nacional de Promoción Científica y Tecnológica (ANPCyT) from Argentina. This work was partially supported by Science Foundation Ireland under grant no. SFI/13/IA/1886 and grant no. 12/RC/2302 for the MaREI Centre for Marine and Renewable Energy.

8 References

[1] Falcao, A.F.O., Henriques, J.C.C.: 'Oscillating-water-column wave energy converters and air turbines: a review', *Renew. Energy*, 2016, **85**, pp. 1391–1424

[2] Korde, U.A., Ringwood, J.V.: '*Hydrodynamic control of wave energy devices*' (Cambridge University Press, Cambridge, 2016)

[3] Ceballos, S., Rea, J., Lopez, I., *et al.*: 'Efficiency optimization in low inertia wells turbine-oscillating water column devices', *IEEE Trans. Energy Convers.*, 2013, **28**, (3), pp. 553–564

[4] Falcao, A.F.O., Henriques, J.C.C., Gato, L.M.C.: 'Rotational speed control and electrical rated power of an oscillating-water-column wave energy converter', *Energy*, 2017, **120**, pp. 253–261

[5] Barambones, O., Cortajarena, J.A., Gonzalez de Durana, J.M., *et al.*: 'A real time sliding mode control for a wave energy converter based on a wells turbine', *Ocean Eng.*, 2018, **163**, pp. 275–287

[6] M'zoughi, F., Bouallègue, S., Garrido, A.J., *et al.*: 'Stalling-free control strategies for oscillating-water-column-based wave power generation plants', *IEEE Trans. Energy Convers.*, 2018, **33**, (1), pp. 209–222

[7] Mishra, S.K., Purwar, S., Kishor, N.: 'An optimal and non-linear speed control of oscillating water column wave energy plant with wells turbine and DFIG', *Int. J. Renew. Energy Res.*, 2016, **6**, (3), pp. 995–1006

[8] Beltran, B., Benbouzid, M.E.H., Ahmed-Ali, T.: 'Second-order sliding mode control of a doubly fed induction generator driven wind turbine', *IEEE Trans. Energy Convers.*, 2012, **27**, (2), pp. 261–269

[9] Alberdi, M., Amundarain, M., Garrido, A.J., *et al.*: 'Complementary control of oscillating water column-based wave energy conversion plants to improve the instantaneous power output', *IEEE Trans. Energy Convers.*, 2011, **26**, (4), pp. 1021–1032

[10] Amundarain, M., Alberdi, M., Garrido, A.J., *et al.*: 'Modeling and simulation of wave energy generation plants: output power control', *IEEE Trans. Ind. Electron.*, 2011, **58**, (1), pp. 105–117

[11] Garrido, A.J., Garrido, I., Amundarain, M., *et al.*: 'Sliding-mode control of wave power generation plants', *IEEE Trans. Ind. Appl.*, 2012, **48**, (6), pp. 2372–2381

[12] Barambones, O., Gonzalez de Durana, J., Calvo, I.: 'Adaptive sliding mode control for a double fed induction generator used in an oscillating water column system', *Energies*, 2018, **11**, (11), p. 2939

[13] Utkin, V.I.: 'Variable structure systems with sliding modes', *IEEE Trans. Autom. Control*, 1977, **22**, (2), pp. 212–222

[14] Utkin, V.I., Gulder, J., Shi, J.: '*Sliding mode control in electro-mechanical systems*' (Taylor and Francis, London, 1999)

[15] Sira-Ramirez, H.On the dynamical sliding mode control of nolinear systems', *Int. J. Control.*, 1993, **57**, (5), pp. 1039–1061

[16] Bartolini, G., Fridman, L., Pisano, A., *et al.*: '*Modern sliding Mode control theory*'. *Lecture Notes in Control and Information Sciences*, vol. **375**, (Springer, Berlin, Heidelberg, 2008)

[17] Fridman, L., Moreno, J., Iriarte, R., *et al.*: 'Sliding modes after the first decade of the 21st century'. *Lecture Notes in Control and Information Sciences*, vol. **412**, (Springer, Berlin Heidelberg, 2012)

[18] Bandyopadhyay, B., Janardhanan, S., Spurgeon, S.K., *et al.*: 'Advances in sliding mode control'. *Lecture Notes in Control and Information Sciences*, vol. **440**, (Springer, Berlin Heidelberg, 2013)
[19] Barbot, J.P., Plestan, F., Fridman, L. (Eds.): '*Recent trends in sliding mode control*' (Institution of Engineering and Technology, United Kingdom, 2016)
[20] Li, S., Yu, X., Fridman, L., *et al.*: 'Advances in variable structure systems and sliding mode control theory and applications', in '*Studies in systems, decision and control*, vol. **115**, (Springer International Publishing, Cham, 2018)
[21] Levant, A.: 'Sliding order and sliding accuracy in sliding mode control', *Int. J. Control.*, 1993, **58**, (6), pp. 1247–1263
[22] Bartolini, G., Pisano, A., Punta, E., *et al.*: 'A survey of applications of second-order sliding mode control to mechanical systems', *Int. J. Control.*, 2003, **76**, (9/10), pp. 875–892
[23] Shtessel, Y., Edwards, C., Fridman, L., *et al.*: 'Sliding mode control and observation', in Shtessel, Y., Edwards, C., Fridman, L., Levant, A. (Eds.) (Springer, New York, New York, 2013)
[24] Folley, M.: 'The wave energy resource', in PecherJens, A., Kofoed, P. (Eds.): *Handbook of ocean wave energy* (Springer International Publishing, Switzerland, 2016) pp. 43–79
[25] Falnes, J.: 'A review of wave-energy extraction', *Mar. Struct.*, 2007, **20**, (4), pp. 185–201
[26] Nolan, G., Ringwood, J.V., Holmes, B.: 'Short Term Wave Energy Variability off the West Coast of Ireland', 2007
[27] Shehata, A.S., Xiao, Q., Saqr, K.M., *et al.*: 'Wells turbine for wave energy conversion: a review', *Int. J. Energy Res.*, 2017, **41**, (1), pp. 6–38
[28] Falcão, A.F.O., Gato, L.M.C., Nunes, E.P.A.S.: 'A novel radial self-rectifying air turbine for use in wave energy converters', *Renew. Energy*, 2013, **50**, pp. 289–298
[29] Ghisu, T., Puddu, P., Cambuli, F.: 'A detailed analysis of the unsteady flow within a wells turbine', *Proc. Inst. Mech. Eng. Part A J. Power Energy*, 2017, **231**, (3), pp. 197–214
[30] Abad, G., Lopez, J., Rodriguez, M., *et al.*: '*Doubly fed induction machine*' (John Wiley & Sons, United Kingdom, 2011)
[31] Lekube, J., Garrido, A.J., Garrido, I.: 'Rotational speed optimization in oscillating water column wave power plants based on maximum power point tracking', *IEEE Trans. Autom. Sci. Eng.*, 2017, **14**, (2), pp. 681–691
[32] Sabanovic, A.: 'Variable structure systems with sliding modes in motion control - A survey', *Ind. Inf. IEEE Trans.*, 2011, **7**, (2), pp. 212–223
[33] Levant, A.: 'Higher-order sliding modes, differentiation and output-feedback control', *Int. J. Control.*, 2003, **76**, (9), pp. 924–941
[34] Boiko, I., Fridman, L., Pisano, A., *et al.*: 'Analysis of chattering in systems with second-order sliding modes', *IEEE Trans. Autom. Control*, 2007, **52**, (11), pp. 2085–2102
[35] Bartolini, G., Ferrara, A., Levant, A., *et al.*: 'Variable structure control of nonlinear sampled data systems by second order sliding modes', in Young, K.D., Ozguner, U. (Eds.) *Variable structure systems, sliding mode and nonlinear control* (Springer, United Kingdom, 1999), pp. 329–350